Supplemental Information

Supplemental Figure S1. Top canonical pathways associated with WSB1 expression. differentially expressed genes associated with canonical pathway in INGENUITY pathway analysis. Total RNA were extracted from 56 pairs of fresh-frozen (FF) primary never smoker lung adenocarcinomas and analyzed by WSB1 status using INGENUITY pathway analysis (see Supplemental Experimental Procedures.)

Supplemental Figure S2. Top biological functions associated with WSB1 expression. Gene expression profiles using total RNA from 56 pairs of fresh-frozen (FF) primary never smoker lung adenocarcinomas and analyzed by WSB1 status using INGENUITY pathway analysis (see Supplemental Experimental Procedures.)

Supplemental Figure S3. Metastasis-free survival in breast and colon cancer patients. (*A-C)* Kaplan–Meier graph of (*A*) metastatic human breast cancer, (*B*) breast cancer metastasis to brain and (*C*) metastatic colon cancer patients stratified according to high or low expression levels of WSB1 (PROGgene).

Supplemental Figure S4. WSB1 interacts and negatively correlated with pVHL. (*A*) Co-immunoprecipitation (Co-IP) of exogenous HIF-1α (HA), pVHL (HA) and WSB1 (Myc) from extracts of HEK 293T cells. * indicates non-specific band. (*B*) Five lung, six pancreatic, four breast cancer cell lines and normal MCF10A cells were analyzed by immunobloting for indicated proteins.

Supplemental Figure S5. HIF-1α level and target gene's expression were decreased in cells depleted of WSB1. (*A*) Representative images of HIF-1α protein expression in HeLa cells. Cells were transfected with *WSB1* shRNA (#1 or #2) (GFP positive) and then stained with DAPI (blue for DNA) and anti-HIF-1α (red). Infected cell by *WSB1* shRNA are indicated by white arrowheads. The scale bar represents 10 μm. (*B*) Cells were infected with *WSB*1 shRNA (#2) and then collected for qPCR analysis. *, *P< 0.05*, **, *P< 0.01* versus *Control* shRNA by one-way ANOVA.

Supplemental Figure S6. The correlation between WSB1 and HIF target genes expression in metastatic colon and urinary bladder cancer patients (GEO data set. Table S1)

Supplemental Figure S7. WSB1 interacts with pVHL in hypoxia mimic conditions. (*A*) Cells were treated with $CoCl_2$ and MG132 and then collected for immunoprecipitation (IP) and immunoblot analysis. (*B*) Cells were infected with *HIF-1α* shRNA and then collected in hypoxic or normoxic conditions. S.E. , short exposed; L.E., long exposed. (*C*) HIF-1α, HIF-2α, pVHL and WSB1 protein levels were examined after $CoCl_2$ treatment without MG132.

Supplemental Figure S8. WSB1 promotes cancer cell invasion and migration by enhance HIFs. (*A*) Cells were transduced with or without the viral vectors indicated and collected for immunoblot analysis. (*B*) Trans-well invasion assay of 786-O or 786-O/VHL cells stably expressing the indicated shRNAs or plasmids. The plot shows quantification of the area covered by the invasion cells, relative to the control. The results represent the means (±S.E.) of three independent experiments performed in triplicate. **, *P< 0.01* versus vector virus injected cells; *, *P< 0.05* versus *Control* shRNA infected cells by one-way ANOVA. (*C*) Quantification of wound-healing assays of 786-O or 786-O/VHL cell lines stably transfected

with the indicated plasmids or shRNA. The mean and s.d. of one representative experiment, out of three independent experiments performed in triplicate, are shown (***, *P< 0.001* versus vector virus injected cells by one-way ANOVA). (*D*) Representative images in Supplemental Figure S8C. (*E* and *F*) Lentiviral-driven shRNA was used to deplete endogenous WSB1 and rescue with an RNAi-resistant *WSB1 (Wt* or *ΔSOCS)* in MDA-MB-231 cells. (E) HIF-1α activity. The results represent the means (±S.E.) of three independent experiments performed in triplicate. ***, *P< 0.001* versus *Control* shRNA virus infected cells; ****, *P< 0.0001* versus *WSB1* shRNA infected cells by one-way ANOVA. (F) Cells as in (E) were then collected for immunobloting with the indicated proteins. Exo, Exogenous; Endo, Endogenous. (*G*) Representative images of wound healing experiments. Lentiviral-driven shRNA was used to deplete endogenous WSB1 and rescue with an RNAi-resistant *WSB1 (Wt* or *ΔSOCS)* in RCC4/VHL cells.

Supplemental Figure S9. WSB1 regulates HIF-1α in a HIPK2 independent manner. Left: Cells were infected with indicated shRNA and were assayed by wound healing experiments. Right: The expression of indicated proteins was examined by immunobloting.

Supplemental Figure S10. WSB1 promotes cancer cell metastasis and negatively correlated with pVHL in tail vein metastasis. (*A*) Lung colonization assay of mice intravenously injected with B16F10 cells stably infected with the indicated viral construct or shRNA. Top: Representative lung organs were shown. Middle: The plot shows the number of metastatic foci per section. **, *P< 0.01* by one-way ANOVA. Bottom: Cells as in (Top) were then collected for immunoblot analysis. Exo, Exogenous; Endo, Endogenous. (*B-D*) Lung or liver colonization assay of mice intravenously injected with B16F10 cells stably infected with the indicated viral construct or shRNA. (*B*) Representative lung organs or liver were shown. (*C*)

The plot shows the number of metastatic foci per section. (*D*) Cells as in (B) were then collected for immunoblot analysis. Exo, Exogenous; Endo, Endogenous. *, $P< 0.05$, **, $P< 0.01$, ***, $P< 0.001$ versus control cells by one-way ANOVA.

Supplemental Table 1. The GEO Dataset.

Supplemental Table 2. Differentially expressed meta_related genes by WSB1 status in never-smoker lung adenocarcinoma.

Supplemental Methods

Plasmids .

Myc-tagged WSB1 (empty and WT, ΔWD1-2, ΔWD1-3, ΔN, ΔSOCS and ΔC) were kindly provided by Dr. Cheol Yong Choi (Sungkyunkwan University, Korea)(Choi et al. 2008). HA-tagged HIF-1α and HA-tagged VHL (Wt, C162F and R167W) were obtained from Addgene.

*Transient Transfection and Stable Transduction***.**

shRNAs were infected using Lipofectamine 2000 reagent (Invitrogen). Human WSB1, mouse WSB1, HIF-1α, HIPK2, Cullin2 and 5 were obtained from Sigma-Aldrich and Open Biosystems.

WSB1 shRNA (human) : Open Biosystems

5'- TGCTGTTGACAGTGAGCGCGGAGTTTCTCTCGTATCGTATTAGTGAAGCCACAGA TGTAATACGATACGAGAGAAACTCCATGCCTACTGCCTCGGA -3'

5'- TGCTGTTGACAGTGAGCGCGCTGTAAAGTGCAAGGAAATTTAGTGAAGCCACAG ATGTAAATTTCCTTGCACTTTACAGCATGCCTACTGCCTCGGA -3'

WSB1 shRNA (Mouse) : Sigma-Aldrich

5'- ACATGAGCTGCTGCTATATAT -3'

5'- GCTTACTCCTTGTATCAGCTT-3'

HIF-1 α shRNA (Mouse) : Sigma-Aldrich

5'-GTGATGAAAGAATTACCGAAT -3'

5'- TGCTCTTTGTGGTTGGATCTA-3'

HIPK2 shRNA (Mouse) : Open Biosystems

5'- GCTGTTGACAGTGAGCGACGAGTCAGTATCCAGCCCAATTAGTGAAGCCACA

GATGTAATTGGGCTGGATACTGACTCGGTGCCTACTGCCTCGGA -3’

5’-GCTGTTGACAGTGAGCGAGGAGAGTGCCGATGACTATAATAGTGAAGCCACA

GATGTATTATAGTCATCGGCACTCTCCGTGCCTACTGCCTCGGA -3’

Culllin 5 shRNA (human) : Sigma-Aldrich

5’-GCTAGAATGTTTCAGGACATA -3’

5’-CGCTGTATTGTTTGCATGGAA -3’

5’-GCAGACTGAATTAGTAGAAAT -3’

5’-GCAGTAAACTTGCCAAATATA -3’

5’-GCCATCAAGATGATACGGCTT -3’

Culllin 2 shRNA (human) : Sigma-Aldrich

5’-GCAAGCTACATCGGATGTATA -3’

5’-GCCCTTATTCAAGAGGTGATT -3’

5’-CGTTTGCAGTTGATGTGTCTT -3’

5’-CCCTTGGAGAAAGACTTTATA -3’

5’-GCAGACTATATGGACTGCTTA -3’

For transient overexpression studies, DNA plasmids were transfected using Lipofectamine 2000 reagent (Invitrogen). Stable overexpression and silencing were obtained by transducing MDA-MB-231 cells, HEK 293T, HEK 293, RCC4, RCC4/VHL, 786-O, 786-O/VHL and H1299 cells with retroviral or lentiviral vectors. The efficiency of knockdown or overexpression was controlled by Western Blotting.

Migration and Invasion Assays.

For migration assays (wound healing assays), cells were seeded in 6-well plates at a density of 15 % / well and grown until confluence (around 3 days). And then complete medium replaced by serum-free medium, for 24 h. Confluent cells (monolayer) was scraped with a P200 tip in each well (3 lines/well), the medium was replaced with complete medium. After 24 ~ 48 h the cells were fixed with 3.7 % Paraformaldehyde. Photographs were obtained at 0, 1 and 2 days. Cell migration was quantified by counting inside the scratch (at time 0 as standard) in each different fields of the wound.

For matrigel invasion assays, RCC4 or RCC4/VHL and 786-O or 786-O/VHL cells were infected with shRNAs in 10cm dishes. After 8 h, the medium was changed to serum-free medium and grown until ~80 % confluence. Cells were seeded in 24-well invasion chamber (Corning, 354480). Each sample was plated in triplicate (500,000 cells/ insert). All protocol was followed as recommended standard protocol. To measurement of cell invasion, the filter was stained with 0.2 % Crystal Violet and invasion cells were counted.

Coimmunoprecipitation Assays, Immunobloting and Antibodies.

To study endogenous WSB1/pVHL binding, the cells were treated with or without 10 μM MG 132 (Sigma) for 2 hours. Cells was lysed by sonicator in NETN buffer (20 mM Tris-HCl, pH 8.0, 100 mM NaCl, 1mM EDTA, 0.5 % Nonidet P-40) containing 50 mM b-glycerophosphate,10mM NaF, and 1 mg/ml each of pepstatin A and aprotinin, freshly supplemented with protease inhibitor cocktail (Roche). Prior to immunoprecipitation, protein A-bound Agarose beads were incubated overnight with pVHL (Cell signaling, #2738), WSB1 antibody (Abcam, ab68953; Sigma, HPA003293; Proteintech, 1166-1-AP), HIF-1α antibody (Abcam, ab51608), Cullin2 (Abcam, ab166917) and Cullin 5 (Abcam, ab34840) in PBS with 5 % BSA at 4 ℃. We use

ab68953 for most of data (HPA003293 for IHC). We then added to the extracts before immunoprecipitation with protein- A agarose at 4℃ for 4 hours. After three washings in binding buffer, co-purified proteins were analyzed by Western Blotting.

For ubiquitination assays, HEK 293T cells were infected with the indicated shRNAs or HA-tagged VHL (Wt, C162F and R167W) with His-ubiquitin. Before harvesting, cells were treated for 4 hours with proteasome inhibitor 10 μM MG 132 (Sigma). After we performed the ubiquitination assays as described previously (Yuan et al. 2010).

For removing heavy chain, heavy or light-chain-specific anti-mouse and anti-rabbit IgG secondary antibodies were obtained from Jackson Immunoresearch. Rabbit polyclonal antibodies recognizing HIF-2α (Novus, NB100-122), were purchased from Novus. For removing heavy chain, heavy or light-chain-specific anti-mouse and anti-rabbit IgG secondary antibodies were obtained from Jackson Immunoresearch.

Immunofluorescence.

For immunofluorescence staining, HeLa cells were plated on glass cover slips and transfected with the indicated constructs. Cells were then fixed in 3.7 % paraformaldehyde for 10 min at room temperature and stained using standard protocols. Immunofluorescence images were taken using fluorescent microscopy (Nikon Microscope, Melville, New York).

Real time PCR or Reverse Transcription (RT)-PCR of cDNA.

RNA preparation, cDNA, and qRT-PCR were described previously (Lee et al. 2011). The following primers were used:

HIF-1α Forward 5’- CATGGAAGGTATTGCACTGC-3’,

Reverse 5’- CACACATACAATGCACTGTGG -3’,

VEGFA Forward 5’-CCTTGCCTTGCTGCTCTACCTC-3’,

Reverse 5’-TTCTGCCCTCCTCCTTCTGC-3’,

CA90 Forward 5’-CAATATGAGGGGTCTCTGACTACAC-3’,

Reverse 5’- GGAATTCAGCTGGACTGGCTCAGC -3’,

ALDOC Forward 5’- GCGCTGTGTGCTGAAAATCAG-3’,

Reverse 5’- CCACAATAGGCACAATGCCATT-3’,

SAP30 Forward 5’- AGTTGGTTGCCACTTTAGGTC-3’,

Reverse 5’- CCACGTCTCCTAGTGAACACC-3’

GULT1 Forward 5’-TCATCGTGGCTGAACTCTTCAG-3’,

Reverse 5’-TCACACTTGGGAATCAGCCCC-3’,

and *β-actin* sequence were described previously (Lee et al. 2011).

Supplemental References

Choi DW, Seo YM, Kim EA, Sung KS, Ahn JW, Park SJ, Lee SR, Choi CY. 2008. Ubiquitination and degradation of homeodomain-interacting protein kinase 2 by WD40 repeat/SOCS box protein WSB-1. *The Journal of biological chemistry* **283**: 4682-4689.

Lee SB, Kim JJ, Chung JS, Lee MS, Lee KH, Kim BS, Do Yoo Y. 2011. Romo1 is a negative-feedback regulator of Myc. *Journal of cell science* **124**: 1911-1924.

Yuan J, Luo K, Zhang L, Cheville JC, Lou Z. 2010. USP10 regulates p53 localization and stability by deubiquitinating p53. *Cell* **140**: 384-396.

Kim et al., - Supplemental Figure S1

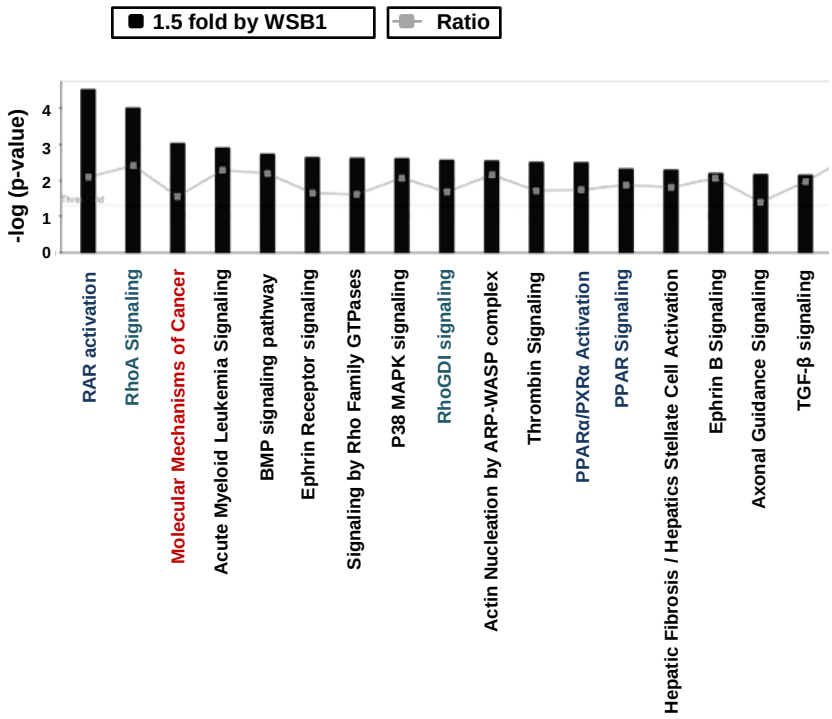

Kim et al., - Supplemental Figure S2

Top Bio Functions

Diseases and Disorders

Name	p-value	# Molecules
Cancer	6.80E-10 - 6.22E-03	703
Infectious Disease	7.62E-08 - 4.42E-03	280
Developmental Disorder	3.76E-07 - 5.70E-03	285
Organismal Injury and Abnormalities	2.94E-06 - 5.65E-03	132
Reproductive System Disease	3.02E-05 - 6.22E-03	246

Molecular and Cellular Functions

Name	p-value	# Molecules
Gene Expression	4.27E-12 - 5.32E-03	401
Cellular Assembly and Organization	5.05E-11 - 6.04E-03	330
Cellular Function and Maintenance	5.05E-11 - 6.38E-03	452
Cellular Growth and Proliferation	9.76E-11 - 6.83E-03	551
Cell Death and Survival	1.60E-10 - 6.04E-03	545

Physiological System Development and Function

Name	p-value	# Molecules
Organismal Survival	2.25E-09 - 3.99E-03	304
Organismal Development	1.21E-08 - 6.83E-03	398
Organismal Functions	1.22E-08 - 4.18E-03	54
Tissue Morphology	1.22E-08 - 6.34E-03	392
Cardiovascular System Development and Function	1.81E-07 - 6.33E-03	248

Top Canonical Pathways

Name	p-value	Ratio
RAR Activation	2.89E-05	36/189 (0.19)
RhoA Signaling	9.48E-05	25/114 (0.219)
Molecular Mechanisms of Cancer	9.12E-04	53/377 (0.141)
Acute Myeloid Leukemia Signaling	1.22E-03	17/82 (0.207)
BMP signaling pathway	1.82E-03	16/80 (0.2)

Top Tox Functions

Assays: Clinical Chemistry and Hematology

Name	p-value	# Molecules
Increased Levels of Red Blood Cells	5.88E-03 - 5.88E-03	18
Increased Levels of Hematocrit	5.89E-02 - 5.89E-02	15
Increased Levels of Albumin	9.92E-02 - 9.92E-02	1
Increased Levels of Alkaline Phosphatase	2.69E-01 - 1.00E00	7

Cardiotoxicity

Name	p-value	# Molecules
Cardiac Dysfunction	5.73E-04 - 6.48E-01	18
Cardiac Hypertrophy	8.71E-04 - 3.00E-01	59
Congenital Heart Anomaly	2.68E-03 - 1.00E00	22
Cardiac Fibrosis	4.16E-03 - 5.45E-01	30
Cardiac Arrythmia	9.83E-03 - 6.04E-01	23

Hepatotoxicity

Name	p-value	# Molecules
Liver Proliferation	1.08E-02 - 3.75E-01	31
Liver Necrosis/Cell Death	1.34E-02 - 6.09E-01	30
Liver Cirrhosis	1.49E-02 - 2.69E-01	23
Liver Cholestasis	3.22E-02 - 5.19E-01	18
Glutathione Depletion In Liver	4.18E-02 - 6.48E-01	6

Nephrotoxicity

Name	p-value	# Molecules
Renal Necrosis/Cell Death	4.16E-03 - 5.28E-01	45
Glomerular Injury	1.49E-02 - 4.11E-01	16
Kidney Failure	3.45E-02 - 1.00E00	24
Renal Damage	5.15E-02 - 5.75E-01	31
Renal Proliferation	5.58E-02 - 4.85E-01	26

Kim et al., - Supplemental Figure S3

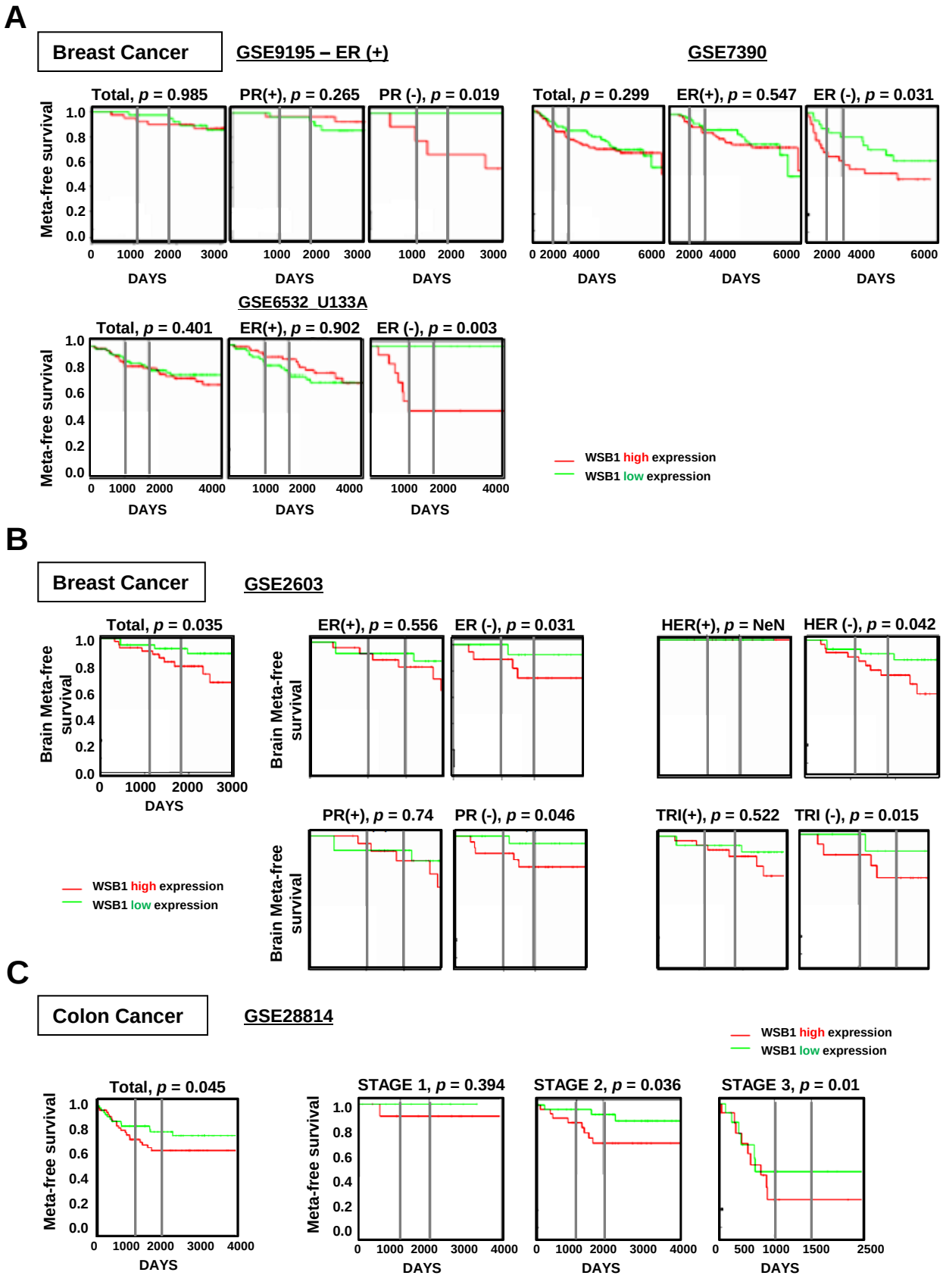

Kim et al., - Supplemental Figure S4

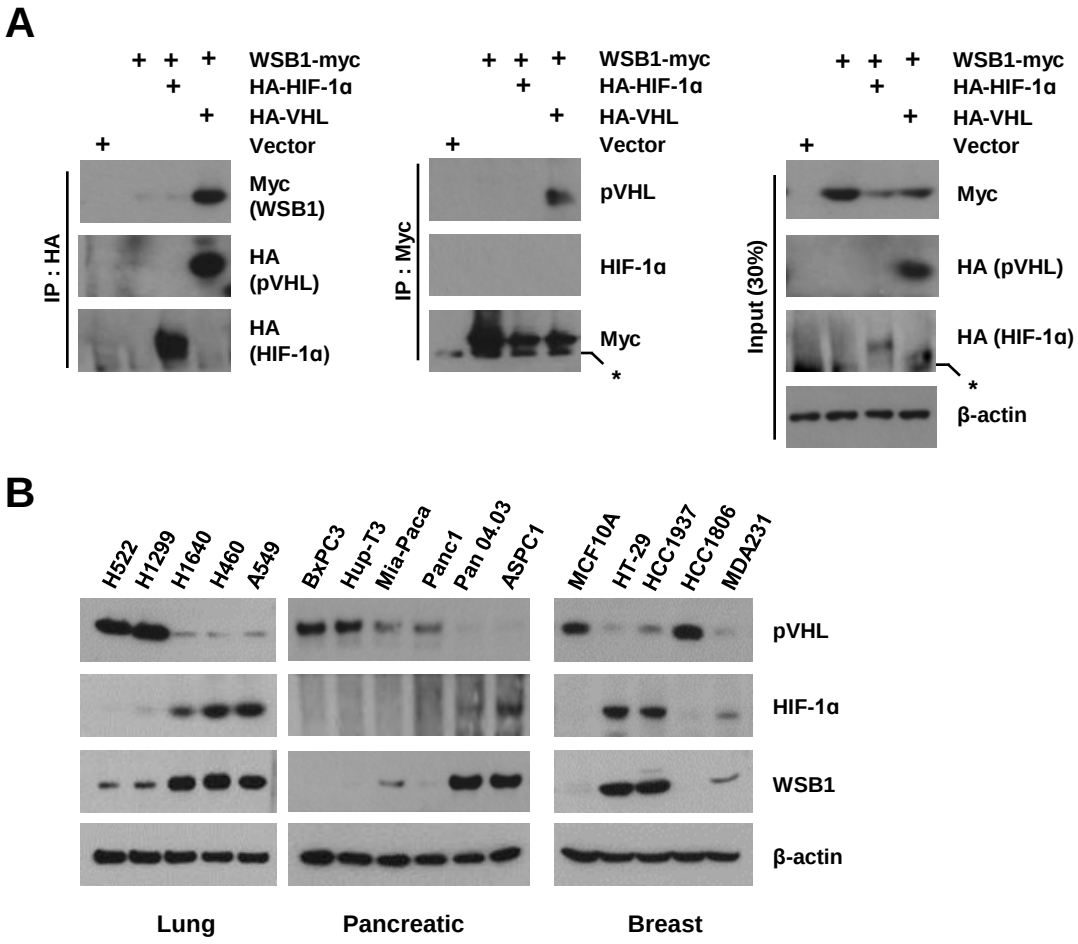

Kim et al., - Supplemental Figure S5

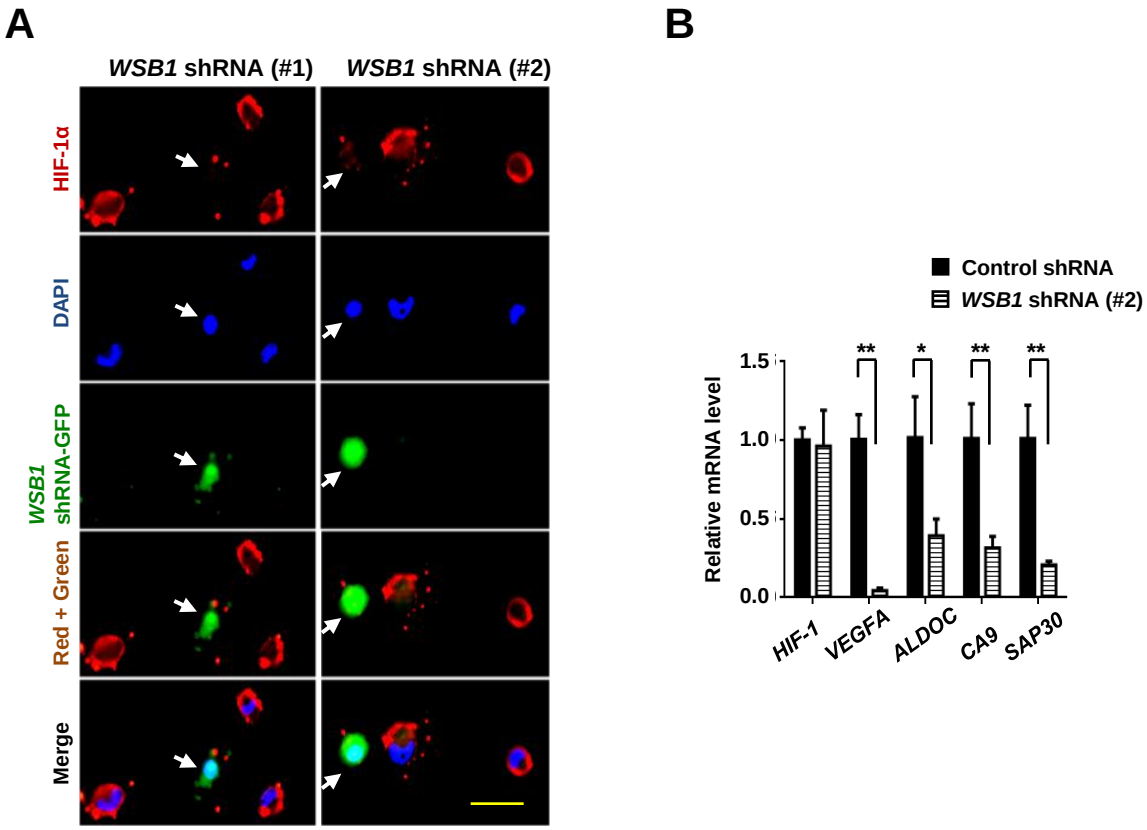

Kim et al., - Supplemental Figure S6

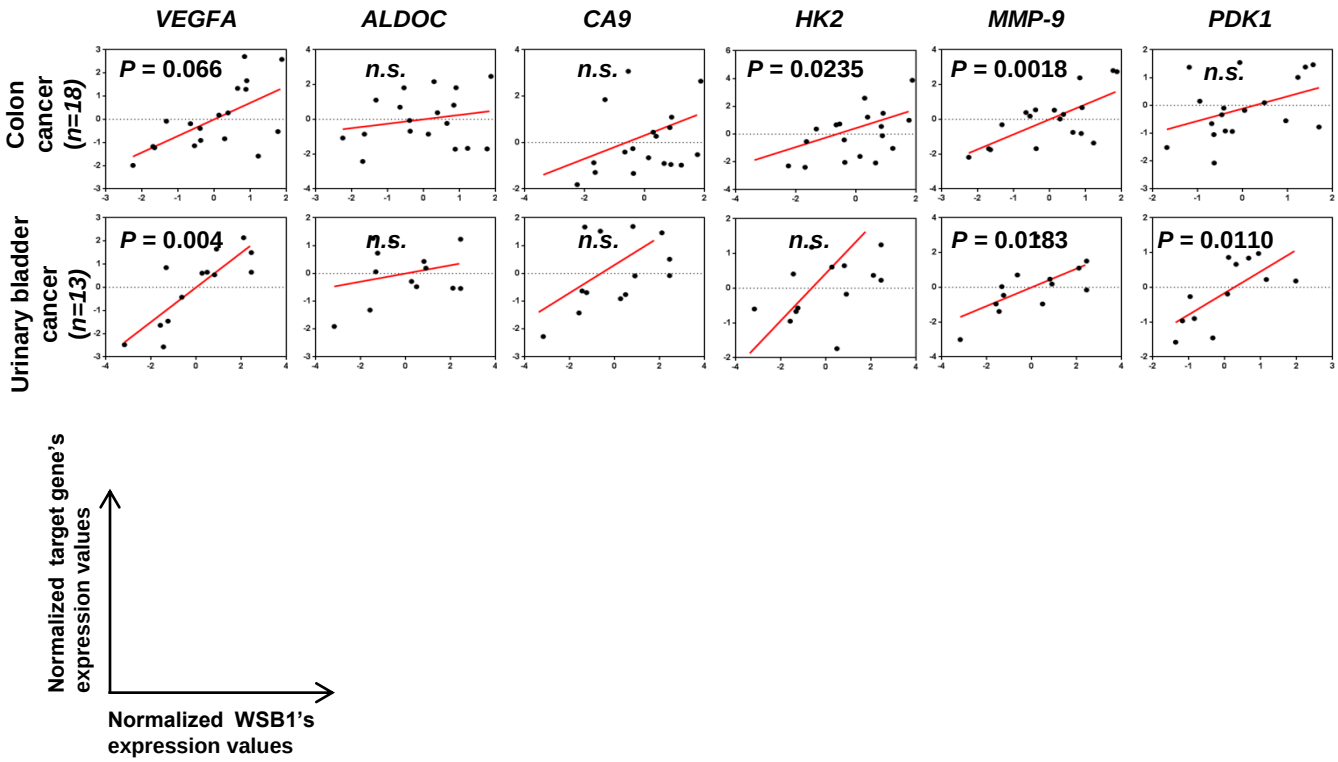

Kim et al., - Supplemental Figure S7

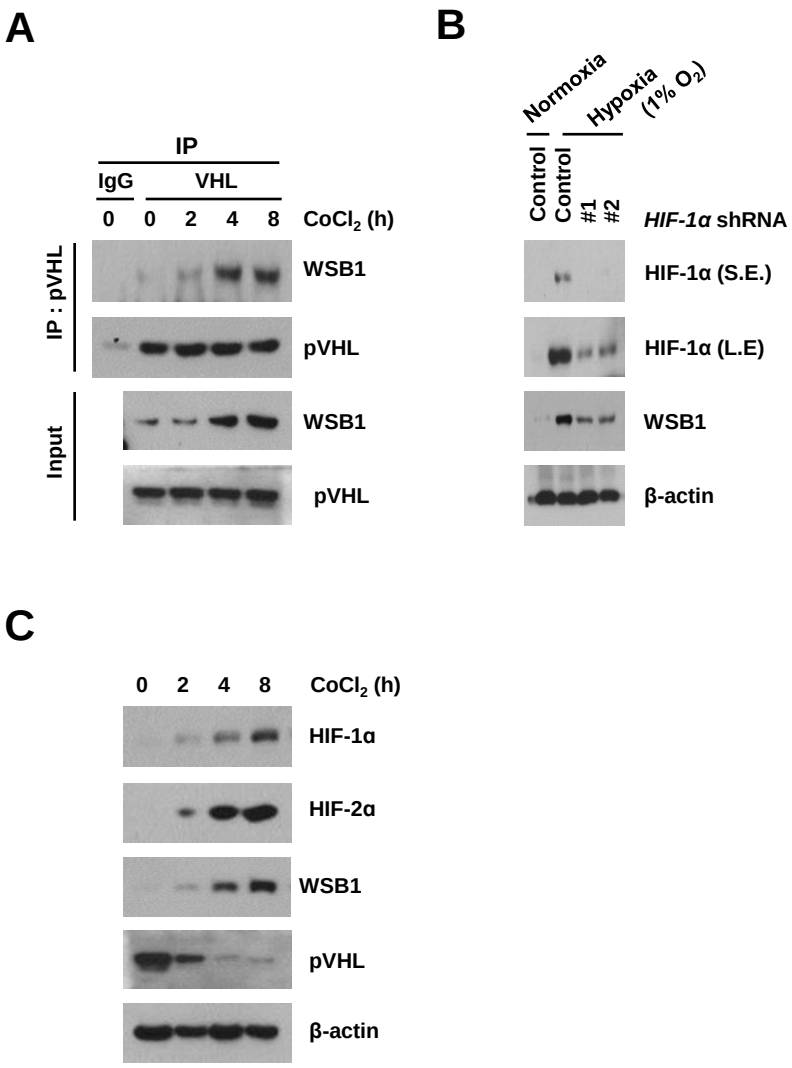

Kim et al., - Supplemental Figure S8

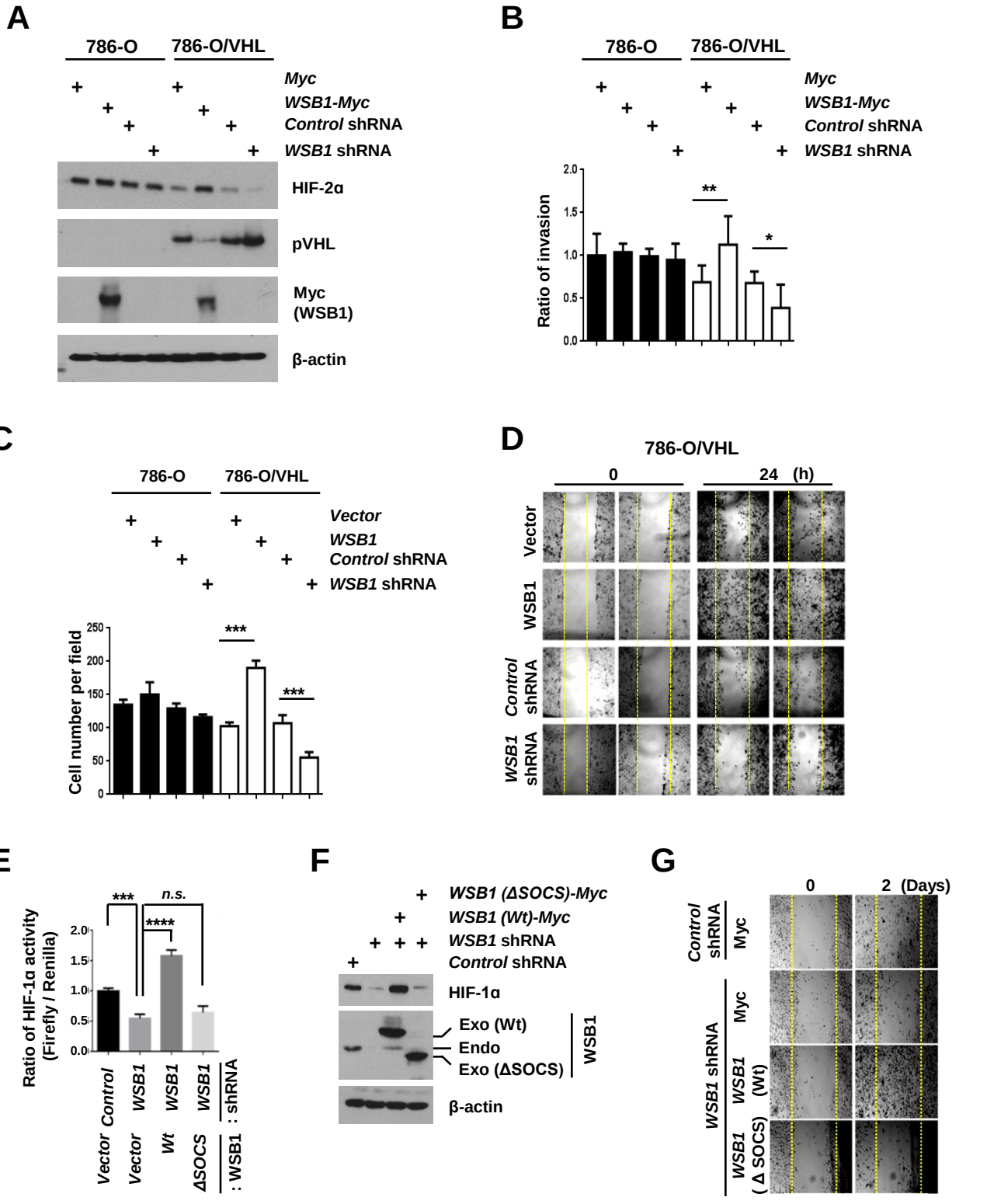

Kim et al., - Supplemental Figure S9

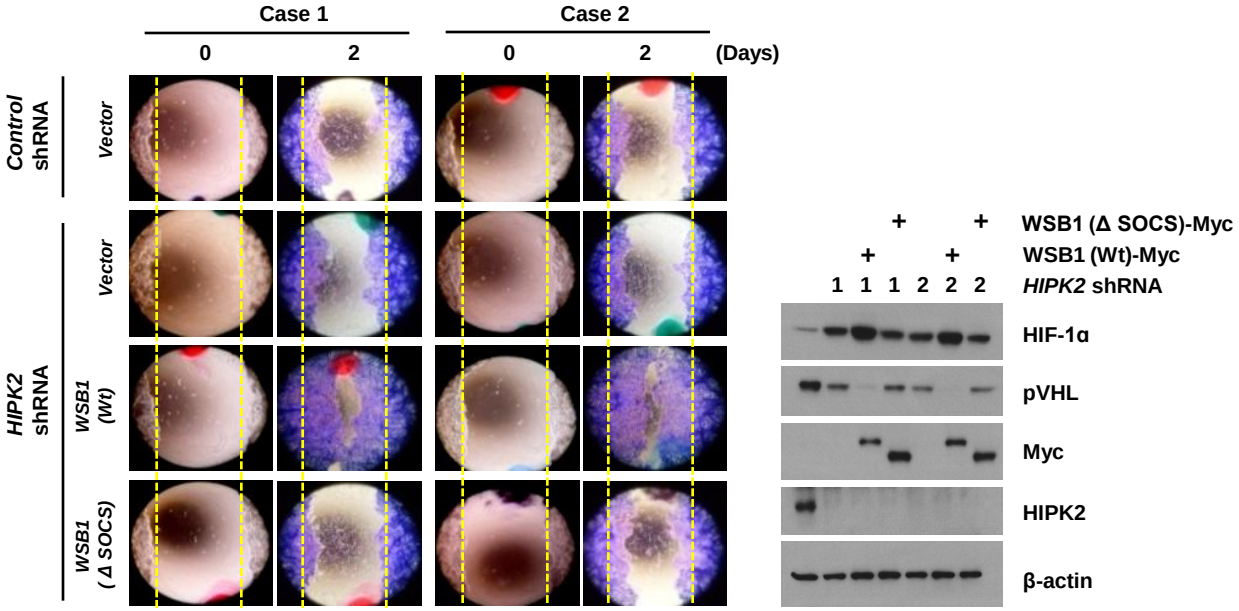

Kim et al., - Supplemental Figure S10

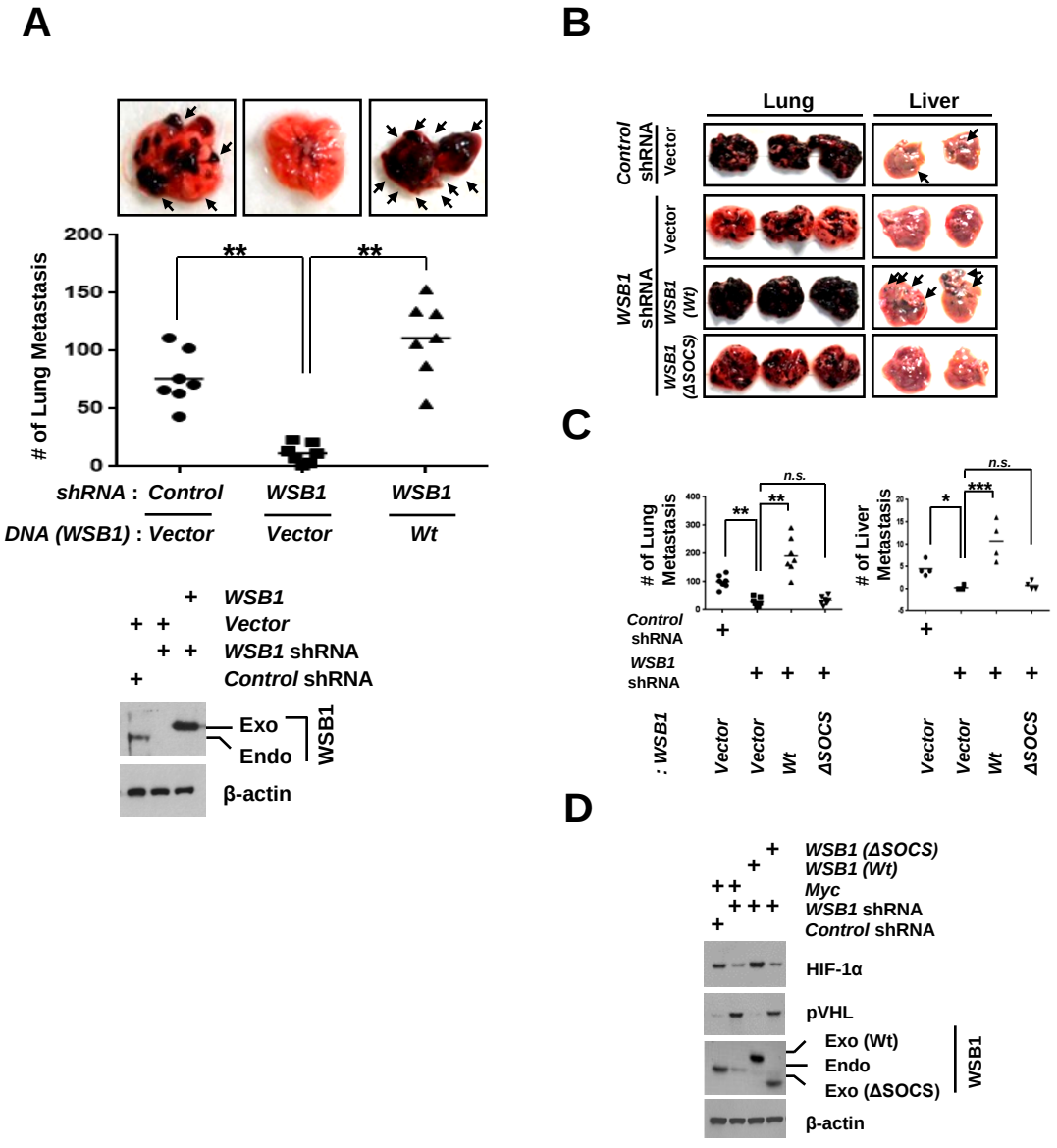

Supplemental Table 1. The GEO Dataset.

Cancer Type	Data set	Platform	Series	#samples	
				Total	Metastasis
Melanoma	GDS3966	GPL96	GSE840	83	50
Prostate	GDS2545	GPL8300	GSE6916	171	25
Synchronous and metachronous liver metastases from colorectal cancer	GDS3501	GPL570	GSE10961	18	18
Carcinoma in situ lesions of the urinary bladder	GDS1479	GPL96	GSE3167	37	13
Breast	GDS3096	GPL96	GSE5847	47	34

Supplemental Table 2. Differentially Expressed Meta_Related Genes by WSB1 Status in Never-Smoker Lung Adenocarcinoma. (Positively related)

ID	Genes in dataset	p-value (Wsb1 status)	Fold-Change (WSB1 High Expression vs WSB1 Low expression)
CXCR4	CXCR4	9.29E-08	2.365
HGF	HGF	6.65E-11	2.175
FABP5	FABP5	3.01E-07	2.069
EGF	EGF	2.84E-06	2.026
ANGPT2	ANGPT2	2.42E-07	1.917
PPM1D	PPM1D	9.39E-09	1.875
ZAP70	ZAP70	5.16E-10	1.844
MMP9	MMP9	3.54E-05	1.84
CA4	CA4	2.49E-06	1.783
VEGFA	VEGFA	1.14E-05	1.749
TACSTD1	EPCAM	2.53E-06	1.702
NUAK1	NUAK1	1.26E-07	1.693
LGALS3	LGALS3	3.69E-10	1.686
HK2	HK2	3.52E-06	1.683
SLC38A6	SLC38A6	2.54E-09	1.667
NT5E	NT5E	4.89E-05	1.651
HTATIP2	HTATIP2	3.40E-05	1.639
OLFML3	OLFML3	6.40E-07	1.617
ANK3	ANK3	1.29E-07	1.609
SP4	SP4	3.76E-09	1.599
CAPN2	CAPN2	6.11E-08	1.595
SLC16A3	SLC16A3	8.32E-06	1.591
DLG7	DLGAP5	0.0064403	1.586
CYP1B1	CYP1B1	6.01E-07	1.58
ESR1	ESR1	0.0007115	1.574
TUBE1	TUBE1	2.74E-07	1.572
NDRG1	NDRG1	2.12E-05	1.565
MET	MET	0.0002945	1.561
MMP2	MMP2	6.54E-07	1.556
TGFA	TGFA	0.0001149	1.552
TUBD1	TUBD1	5.82E-08	1.55
CAT	CAT	2.38E-08	1.545
AKR1C3	AKR1C3	0.0002158	1.53
APC	APC	1.52E-07	1.52
CFLAR	CFLAR	8.53E-11	1.519
SELE	SELE	0.0003739	1.512
TUBB2C	TUBB4B	2.89E-07	1.509
ANGPTL4	ANGPTL4	2.33E-05	1.505

Supplemental Table 2. Differentially Expressed Meta_Related Genes by WSB1 Status in Never-Smoker Lung Adenocarcinoma. (Negatively related)

ID	Genes in dataset	p-value (Wsb1 status)	Fold-Change (WSB1 High Expression vs WSB1 Low expression)
NF2	NF2	8.12E-11	-2.454
RASSF3	RASSF3	1.15E-09	-2.291
TP73L	TP63	0.0133901	-1.868
TP53	TP53	1.86E-05	-1.817
SDC1	SDC1	3.37E-07	-1.792
KISS1	KISS1	0.0031178	-1.732
WWOX	WWOX	6.83E-11	-1.714
NLRP1	NLRP1	3.05E-05	-1.669
SCUBE2	SCUBE2	0.0156027	-1.641
DFFB	DFFB	4.22E-07	-1.637
REV3L	REV3L	3.55E-05	-1.634
LGR4	LGR4	0.007748	-1.581
IL1RL1	IL1RL1	0.0191785	-1.547
PPARD	PPARD	5.90E-05	-1.53
STAB2	STAB2	0.0215461	-1.53
GREM2	GREM2	0.0113608	-1.519